

Received February 11, 2019, accepted February 23, 2019, date of publication March 1, 2019, date of current version March 20, 2019.

Digital Object Identifier 10.1109/ACCESS.2019.2902386

Unmanned High-Rise Façade Cleaning Robot Implemented on a Gondola: Field Test on 000-Building in Korea

SUNGKEUN YOO¹, INHO JOO¹, JOOYOUNG HONG¹, CHANGMIN PARK², JONGWON KIM¹, HWA SOO KIM¹, (Member, IEEE), AND TAEWON SEO², (Member, IEEE)

¹School of Mechanical and Aerospace Engineering, Seoul National University, Seoul 08826, South Korea

²School of Mechanical Engineering, Hanyang University, Seoul 04763, South Korea

³School of Mechanical System Engineering, Kyonggi University, Suwon 16227, South Korea

Corresponding authors: Hwa Soo Kim (hskim94@kgu.ac.kr) and Taewon Seo (taewonsoe@hanyang.ac.kr)

This work was supported by the National Research Foundation of Korea (NRF) Grant funded by the Ministry of Science and ICT for First-Mover Program for Accelerating Disruptive Technology Development under Grant NRF-2018M3C1B9088328.

ABSTRACT Façade cleaning is very difficult and dangerous work for human workers. The automation of façade cleaning is considered a large market with significant potential, and it is also considered a market that needs to be replaced by a robotic solution. Several researchers have previously attempted to replace the façade cleaning task by a semi-automated device; however, there is no effective solution yet on the market. In this paper, we share our experiences involving the unmanned façade cleaning robot equipped on a gondola. The robot is composed of a two-degree of freedom robotic manipulator and a cleaning device. The cleaning device sprays a cleaning solution, brushes the solution, and retrieves the solution by suction with a squeegee. A robust controller is used to operate the robot manipulator in order to control the force and position of the cleaning device to the wall. The robot is tested on the 63-building, which is the most popular high-rise building in Korea, and the successful results are obtained with respect to the cleaning performance, with some problems requiring further improvements. From the field test, we find the potential to commercialize the robotic platform, as well as some information to improve the robot's performance. We believe that the information on the cleaning experiment may be helpful for field robot researchers.

INDEX TERMS Façade cleaning, 2-DOF manipulator, cleaning device, robust control, high-rise building.

I. INTRODUCTION

Façade cleaning is very difficult and dangerous work for human workers. As the number of high-rise buildings increases, there is an increased need for façade cleaning solutions. Many researchers have attempted to develop façade cleaning robots that will replace human workers, but to date, there is no effective and popular solution on the market [1]–[3] owing to their limited mobility, cleaning performance, safety, and adaptability for various types of buildings. Because façade cleaning robots have a large potential market, and are required to replace dangerous human work, many researchers are currently trying to develop reliable solutions, especially for the Chinese market [4].

The associate editor coordinating the review of this manuscript and approving it for publication was Hui Xie.

Wall-climbing robots are the primary platform for the development of a façade cleaning robot that results in a stable mobility on the façade surface. From bio-inspiration to magnetic devices [5]–[8], many different functions are used to design wall-climbing robots, which can be used mainly to clean façades made by glass surfaces. Recently, many engineering solutions involve the use of wire and rope [2], and the guide rail infrastructure is implemented in advance in order to simplify the movement for a façade cleaning robot [9]. By using an effective engineering solution to realize motion on a façade, the reliability of the façade cleaning robots is increased significantly.

Cleaning devices are also very important components when cleaning a façade, and are incorporated into the designs of wall-climbing robots. There have been many studies to develop reliable cleaning solutions. The use of brushes is one of the methods employed to clean large spaces in a short time,

and there are studies to control the force and position simultaneously for the successful cleaning of glass surfaces [10]. The use of a squeegee is a popular approach to cleaning a glass surface by wiping the surface, and there are some reliable products in the market [11]. The use of a pad is also popular for cleaning glass surfaces, and this approach is optimal for cleaning small surfaces in particular, but it needs to be replaced after use [12]. Diatomite is also commonly used when cleaning high-rise buildings.

By augmenting wall-climbing robots with cleaning devices, there are some commercially available façade cleaning robots on the market. An example is Skypro, which uses a wire/rope mechanism to climb a façade, and then uses a brush to clean it [1]. IPC Eagle is a similar device employed to clean a façade, and it adds a thruster to generate an attaching force to the façade using the same climbing and cleaning mechanism as Skypro [3]. Windowmate, Hobot, and Winbot are representative examples of small-size glass-cleaning robots that utilize magnetism and vortex suction for attachment to the surface, and they use the fiber pads to clean the surface [12]–[14]. While there are several commercial products, there are no dominant products in the façade cleaning market, especially for high-rise buildings.

This paper aims to develop a façade cleaning robot and to share the developing experience that is more efficient, safer, cheaper, and cleans better than other existing façade cleaning robots. This robot is equipped on a gondola and cleans a high-rise building façade. The robot is composed of a cleaning device with a spray, brush, and squeegee devices, and it has a 2-DOF manipulator to change the position and orientation of the cleaning device. The impedance control is used for the manipulation in other researches [22]–[24]. The impedance control ensures a constant contact. The contact is controlled by the position based impedance control in [22] and the force tracking impedance control in [24]. In both researches, the proposed impedance control is robust against external disturbances and desired dynamic behavior. For the high quality of the cleaning performance, the feed forward position control and the feedback impedance control methods are used to maintain contact between the cleaning module and the façade. A field test was performed on the 63-building, which is one of the most popular high-rise buildings in Korea [15]. During the design process, we investigated the data of the 63-building, including the gondola system, and the information obtained is presented in this paper. The environmental investigation, parametric design, detailed design, manufacturing, and field test experiences are all presented.

The rest of this paper is organized as follows. Section 2 summarizes existing façade cleaning robots, and analyzes their advantages and disadvantages. Section 3 explains the environmental condition of the field test, and summarizes the requirements for the products. Section 4 presents the overall design of the robot, and the cleaning device and robotic manipulator are explained in detail. Section 5 summarizes the specifications of the assembled robot prototype, and Section 6 explains how the robot is

controlled for successful cleaning. Section 7 summarizes the field test results on the 63-building façade, and the experiences are shared in detail in Section 8. The conclusion and future works are given in Section 9.

II. RELATED RESEARCH

Table 1 lists the classification of the types of façade cleaning robots according to their wall-climbing mechanisms. Note that cleaning devices are typically dependent on the climbing mechanism, such as the use of wires/ropes to perform water cleaning, vortex suction, and pad cleaning.






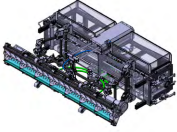
Vortex suction and magnet-based small cleaning robots have disadvantages in terms of the area efficiency and stability/safety margins, while robots have advantages in that they are easy to install and have low manufacturing cost. Because the size of robots is relatively small, the time required to clean a large façade is long, and there is the potential for falling owing to unexpected external forces. A swarm of the vortex suction and magnet-based robots may be a solution to solving the area efficiency, and research on distributed swarm control is required. There is also a need for research to increase the stability in order to ensure safe operation.

Wire/rope-type robots can be classified according to whether the winch is installed on the top of a building or whether it is installed in the robot. The winch-embedded type has an advantage in that it requires relatively simple infrastructure to maintain the rope only, while the winch-less robot requires an additional winch to be installed on top to move the robot. The embedding of the winch in the robot increases the weight of the robot; therefore, when designing an embedded winch-type robot, a light-weight optimal design is very important. It is also important to obtain a reliable design for high-performing winches with a large safety margin. Research is also required into the use of embedded controllers.

Recently, several studies proposed a façade cleaning robot that moves on a pre-implemented guide rail. While this method is very reliable and has good performance when cleaning the façade, the use of this method requires a guide-rail to be implemented on all buildings in advance. This is costly to manufacture and has a limited application area.

The proposed cleaning robot, which is shown on the right side of Table 1, is equipped on a gondola. While the proposed method also has a disadvantage in that a gondola should be implemented in advance, the presence of a gondola on a high-rise building would result in significant advantages in terms of area efficiency, stability, safety, and manufacturing cost. We believe that the proposed cleaning robot will be suitable for high-rise buildings because many high-rise buildings already have installed gondola systems. To achieve good cleaning performance, an appropriate design that considers the environmental conditions of a gondola and building is required, and this research focuses on the 63-building structure.

TABLE 1. Comparison of existing façade cleaning robots.

Climbing Mechanism	Vortex suction	Magnets	Wire/rope (winch installed on top)	Wire/rope (winch embedded in the robot)	Guide rail implemented	Embedded on a gondola
Cleaning	Pad and detergent	Pad and detergent	Water and brush	Water and brush	No information	Water, brush, and squeeze
Pictures						
Name	Winbot[13]	Windowmate[12]	IPC Eagle[3]	Kim et al.[16]	Bisomac[17]	<i>This research</i>
Area efficiency	-	-	+	+	+	+
Cleaning performance	+	-	-	+	+	+
Stability and safety	-	-	+	+	+	+
Need of infrastructure	+	+	- (winch)	+	- (guide-rail)	- (gondola)
Manufacture cost	+	+	-	-	-	+

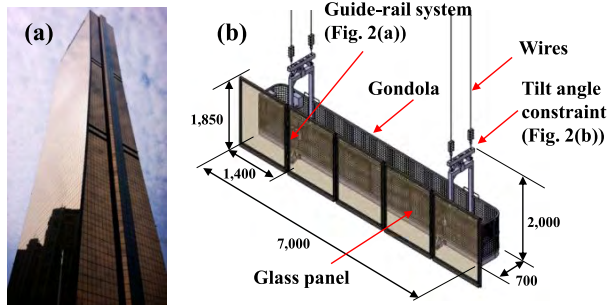


FIGURE 1. (a) External shape of 63-building and (b) 3D model of the gondola with dimensions.

III. ENVIRONMENTAL CONDITION

The 63-building, which is located in Yeouui-do, Seoul, is the most popular high-rise building in Korea. The building was constructed in 1985, and until 2002, it was the highest building in Korea. The building’s height is 250 m, and it has 63 stories. Almost the entire area of the façade is made from glass. Fig. 1(a) shows the shape of the 63-building. It is box shaped with flat surfaces, and the surface has a slope such that its area decreases as the height is increased. Human workers clean the façade four times per year using diatomite fabric rags. It should be noted that the reason for using diatomite rags is that liquid cleaning can result in the re-contamination problem in already-cleaned surfaces while the other surface is being cleaned. Owing to the slope of the building, wind, and disturbances on the gondola, solving the re-contamination problem is important in ensuring that the façade is cleaned well.

There is a gondola on each surface of the 63-building, and they are used for emergencies, maintenance, and cleaning operations. The gondola is shown in Fig. 1(b). The width of each gondola is 7,000 mm, while a single glass panel of the 63-building is 1,400 mm wide, which means that the width of the gondola is five times larger than that of a glass panel. On the wide façade, the 63-building has 36 glass panels in later direction. The winch is installed on the rooftop, and four wires are used to connect the winch and gondola. It is important to note that there are 15-mm rises owing to frames in between glass panels, which should be considered during the cleaning operation.

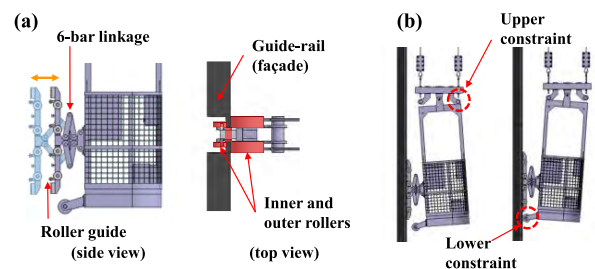


FIGURE 2. (a) Guide-rail system between the gondola and façade, (b) tilt-angle constraint mechanism.

One important part of the gondola is a guide-rail and roller system, as shown in Fig. 2(a). The guide-rail is implemented between glass panels in the 63-building. The gondola and guide-rail are connected by inner and outer rollers with 6-bar linkages to ensure that there is smooth movement vertically,

and to control the distance between the gondola and façade, respectively. The guide-rail constrains the position and orientation of the gondola in order to stabilize the gondola during strong disturbances. Owing to the guide-rail system, the design of a façade cleaning robot is simplified when considering the required DOF for the cleaning operation. The linear stroke of the 6-bar linkage is approximately 200 mm.

There are parts that constrain the tilting angle of the gondola, as shown in Fig. 2(b). On the top of the gondola, a pin-joint with a mechanical stopper is used to vary the tilting angle between -4° and 4° . At the bottom of the gondola, there is also a mechanical stopper between the gondola and façade. These stopper mechanisms are mostly for the safety of the gondola system during operation.

So far, we have investigated the environmental conditions and briefly explained the specifications of the gondola. This information should be used when developing the design requirements in detail, and the design was done to satisfy the requirements. Note that the DOF of the cleaning robot can be simplified based on the gondola specifications, and the re-contamination problem should be solved to design the cleaning device properly. In addition, the small spacing between glass panels should be considered to operate the robot successfully.

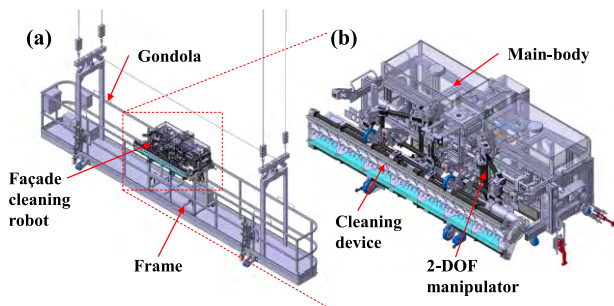


FIGURE 3. Overall configuration of the façade cleaning robot system. (a) The robot positioned on a gondola, and (b) components of the main body, 2-DOF manipulator, and cleaning device.

IV. ROBOT DESIGN

A. OVERALL CONFIGURATION

Fig. 3 shows the system design of the developed façade cleaning robot for the 63-building. The robot is composed of a main body, a 2-DOF manipulator, and a cleaning device. The size of the robot is 1,400 (width) \times 650 – 920 (length, operated by the manipulator) \times 500 (height). The robot can be implemented on a gondola, as shown in Fig. 3, based on the frame structure, and some devices for operations, such as the battery, actuator driver, and controllers are located in the gondola independently. In Fig. 3(a), only one robot is installed for the prototype field test, and five robots can be implemented in series to clean five glass panels simultaneously.

In the main body, some of the equipment is implemented for the cleaning, manipulating, and fixing. The space for clean and used solutions as well as the vacuum suction pump are components for cleaning the main body, whereas active and

TABLE 2. Parameters of façade cleaning robot.

Parameters of the façade cleaning robot	
Width	1400 mm
Height	500 mm
Length	650 mm (Folding, min) 920 mm (Stretching, max)
l	319.9 mm
b	452.3 mm
Weight	18 kgf (Cleaning device) 63 kgf (Main body with manipulator)
Cleaning solution capacity	20 L

passive linear guides and geared motors are the devices for manipulating. A clamping device is attached to the frame to fix the position of the robot. In the next subsections, the 2-DOF manipulator and cleaning device are explained in detail.

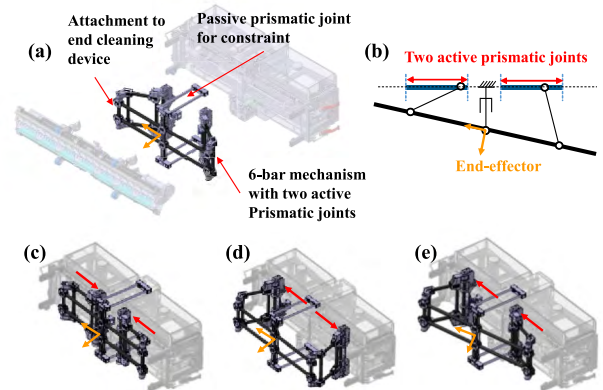


FIGURE 4. Configuration of the 2-DOF robot manipulator. (a) The components of the manipulator, (b) kinematic schematic, (c-e) the workspace of the manipulator in minimum reach (c), maximum reach (d), and the maximum yawing angle (e).

B. 2-DOF ROBOT MANIPULATOR

Fig. 4 shows the configuration of the 2-DOF manipulator used to manipulate the cleaning device. Details of the components are shown in Fig. 4(a). The mechanism is designed using a parallel mechanism to reduce the number of moving parts, increase the payload, and to make the precise motion. The main characteristics employed to design the manipulator for the façade cleaning robot is that the robot needs a large space for the end-effector and high payload of the end-effector. We used a 6-bar mechanism with two active prismatic joints with one passive prismatic joint for constraints, as shown in Fig. 4(b). As a result, the manipulator generates one translation vertical to the façade and one rotation in the yaw direction. Note that two DOF are sufficient to achieve good cleaning performance owing to the constraint mechanism in the 63-building's gondola.

The parametric design of the manipulator is also important to satisfy the requirement. We optimized the kinematic design

TABLE 3. Optimization result.

Parameters	Flow rate	Deflection of squeegee	Deflection of roller fabric brush	RPM of roller fabric brush
Result	0.1 (L/min)	3 (mm)	3 (mm)	200 (rpm)

parameters to maximize the dynamic manipulability under several constraints. Details of the optimal design problem and results are explained in another publication [18].

In Section 3, one of the most important constraints is the workspace of the manipulator, by considering the working range of the guide-rail system in the 63-building. Figure 4(c-e) shows the movement in the workspace of the manipulator with a translation of 270 mm and rotation of 11.85°.

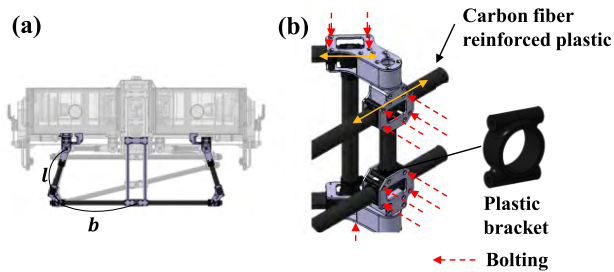


FIGURE 5. a) Link length l and b of the manipulator b) Component of the manipulator joint.

The target workspace of manipulator in Fig. 4 is about the 63-buildings. However, the configuration of the manipulator can be customized according to the workspace of different buildings. Also, there is the algorithm for obtaining the configuration of the optimized manipulator in target workspace [18]. Fig. 5 shows how to change the configuration of the manipulator. In Fig. 5 (a), l and b are the link length of the manipulator. The work space of the manipulator can be changed by adjusting the length of the l and b . In Fig. 5 b), the links are made from Carbon Fiber Reinforced Plastic(CFRP) and plastic bracket by bolting. The link length can be changed by releasing bolts of the CFRP bracket and adjusting position of the bracket.

C. CLEANING DEVICE

The cleaning device is the most important component required to perform successful cleaning. Water-solution cleaning is well known for its high cleaning performance, but its use is not popular in various buildings owing to the re-contamination problem in that the scattered solution in the operation causes the already-cleaned surface to become dirty again. The cleaning device design should solve this re-contamination problem if the water-solution cleaning method is employed.

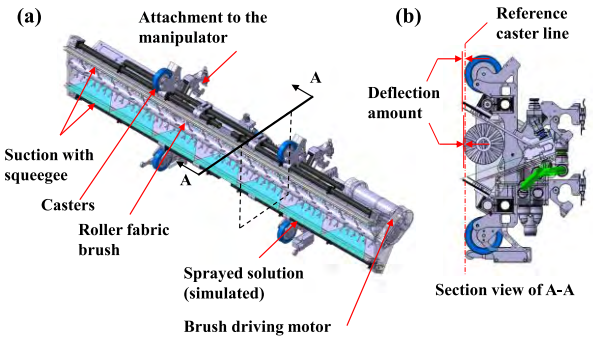


FIGURE 6. Configuration of the cleaning device.

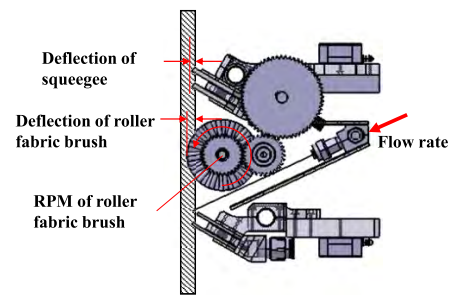


FIGURE 7. Parameters.

Fig. 6 shows the proposed cleaning device design. The device is composed of a spray nozzle, brush, and suction with squeegee. The order of cleaning is as follows: a) the nozzle sprays the solution onto the façade with high pressure, b) the brush rubs the façade using a constant force, and c) the upper squeegee is used to make the final cleaned surface, and d) the lower squeegee block the solution and the contaminants which flow down along the surface, and e) the used solution is retrieved by suction. There are two suctions with the squeegee to cause the operation surface to become isolated during cleaning. The squeegee and the roller brush pressure is This design minimizes the amount of scattered solution, and retrieves almost all the used solution. The squeegee and the roller pressure, roller’s rotation speed, flow rate were optimized in the previous publication to maximize the cleaning performance (Fig.7). The optimized parameters are shown in Table 3 [19]. The squeegee and the roller pressure are related with the deflection. The pressure is important component in cleaning performance [16], [20]. For maintaining the optimized deflection during the cleaning operation, the roller casters are attached above and below the cleaning device. Based on the design, it is expected that the re-contamination problem would be solved, and this will be verified by performing experiments.

V. CONTROL METHOD

A. FORCE TRACKING CONTROL FOR CLEANING

The cleaning device is designed to maintain the optimized deflection amount of squeegees and brush to clean glass panels with proper pressure when the caster rollers move on

glass panels. Therefore, it is very important for the manipulator to keep caster rollers attaching to the glass panels during glass-cleaning. Distance sensors are adopted to measure the distance between cleaning device and glass panels. At the same time, the position-based impedance force control is used to ensure a constant contact force to help all the casters of cleaning device keep good contact with the glass panel.

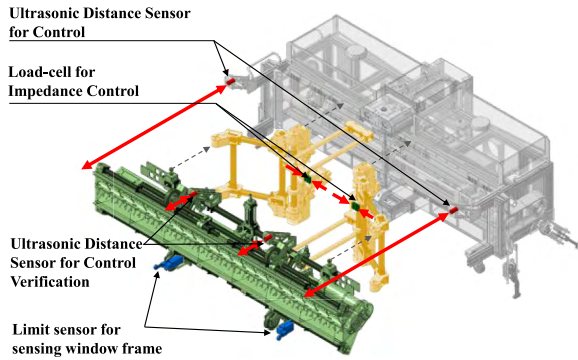


FIGURE 8. Robot sensors.

Fig. 8 shows several sensors of the robot to measure the distance with the aim of avoiding the raised frames between glass panels. Ultrasonic distance sensors are mounted on the robot body to measure the distance as well as tilting angle of the glass panels. 2 load-cells are mounted between the motor and 6-bar linkage mechanism to measure the contact force between the end-effector and the glass panel. 2 limit switch sensors are located next to lower casters for the manipulator to detect the raised frame and detach the cleaning device from glass panels appropriately. Other two ultrasonic sensors are mounted on the end effector to measure the distance from the glass panel.

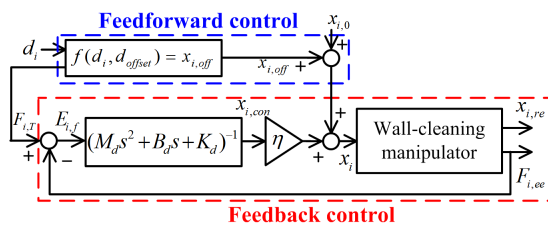


FIGURE 9. Control structure.

The block diagram of force-tracking control framework is shown in Fig. 9. The entire control system consists of two parts. One is the feed forward position control whose goal is to manage the distance between the cleaning device and glass panels with high fidelity. It is noted that at the initial stage of cleaning, the offset distance is required to prevent the cleaning device from colliding with glass panels by minimizing the detrimental effect of position errors of the manipulator and ultrasonic distance sensors. The other is the feedback position-based impedance control loop which produces the additional position input for the manipulator to

drive the cleaning device into glass panels and to generate a desired contact force sufficiently enough to clean glass panels. The detailed control strategy is in details described in Fig. 10.

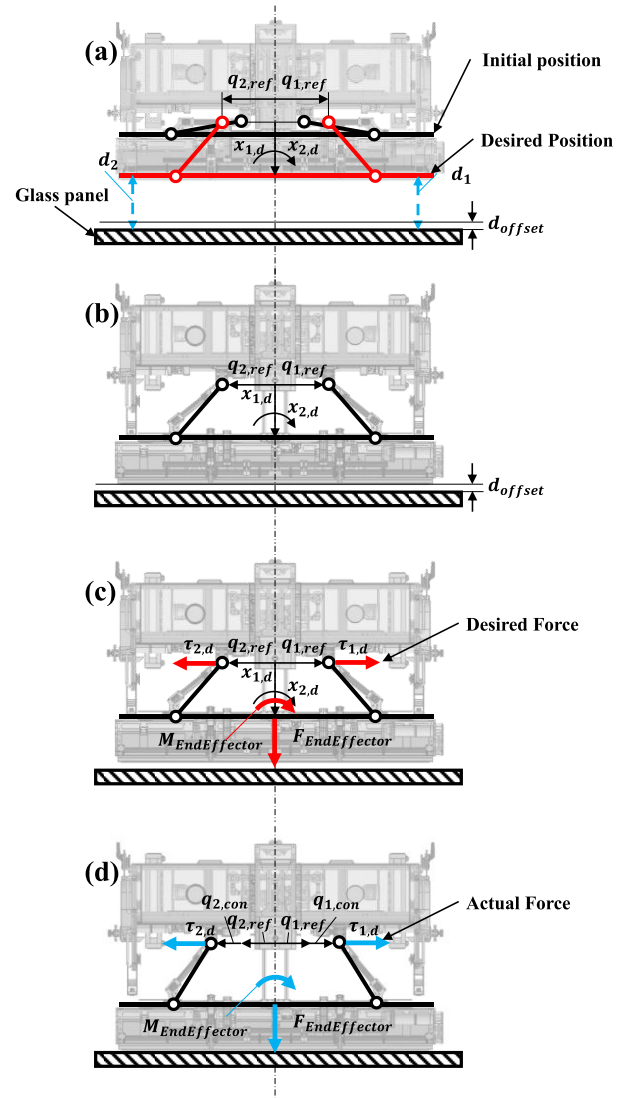


FIGURE 10. Force tracking process.

(a) Measure the distances (d_1, d_2) between left/right-side end of end-effector and the glass panel by ultrasonic distance sensors. Then, calculate the desired left/right-side movement of the end effector ($x_{1,off}, x_{2,off}$) to maintain a constant distance d_{offset} from the glass panel.

(b) Calculate the corresponding input to joint $Q_{off} = (q_{1,off}, q_{2,off})$ by the inverse kinematics of manipulator and move the end-effector by inserting Q_{off} .

(c) Calculate the initial motion of end-effector ($x_{1,0}, x_{2,0}$) to achieve the desired contact force $F_{i,T}$ from the current configuration of manipulator ($x_{i,d}, x_{i,off}, q_{i,off}$). Move the end-effector of manipulator by inserting the corresponding input to joint $Q_0 = (q_{1,0}, q_{2,0})$.

(d) Calculate the additional motion of end-effector $(x_{1,con}, x_{2,con})$ by the position-based impedance control in (1) and (2) [10], which is driven by the force tracking error between the real and desired contact forces $F_{i,ee}$ and $F_{i,T}$. Move the end-effector of manipulator by adding the corresponding input $Q_{con} = (q_{1,con}, q_{2,con})$ to $Q_{off} + Q_0$.

$$M_d \ddot{x}_{i,con} + B_d \dot{x}_{i,con} + K_d(t)x_{i,con} = -E_{i,f} \quad (1)$$

$$\begin{cases} K_d(t) = (k_p E_{i,f} + k_d \dot{E}_{i,f} + k_i \int_0^t E_{i,f}(\tau) d\tau)x_{i,con}^{-1} + k_0 \\ x_i = x_{i,0} + x_{i,off} + \eta x_{i,con} \end{cases} \quad (2)$$

where M_d , B_d and $K_d(t)$ denote the target mass, damper and stiffness of impedance model, respectively. $E_{i,f}$ is the force tracking error of motor defined by $E_{i,f} = F_{i,T} - F_{i,ee}$, where $F_{i,T}$ and $F_{i,ee}$ are the desired and real contact forces of end-effector, respectively. k_0 and $x_{i,0}$ are the initial target stiffness of impedance model and initially desired position of end-effector, respectively. k_p , k_d and k_i are the positive PID control gains and η is the positive scaling factor. Note that as shown in Fig. 8, the load cell sensors are located at the motor to directly measure the force exerted by the motor. Assuming that the gondola moves slowly, the real contact force at the end-effector is obtained by using $F_{i,ee} = J^{-T} \tau_{i,T}$ where J is the Jacobian matrix of proposed manipulator.

Without loss of generality, it is assumed that the contact force can be expressed by $F_{i,ee} = -k_e(x_{i,re} - x_e)$ with the stiffness k_e and position x_e of glass panel and the position of end-effector $x_{i,re}$, respectively. Since the force tracking error is expressed by $E_{i,f} = F_{i,T} + k_e(x_{i,re} - x_e)$, the real position of end-effector, its 1st and 2nd derivatives can be approximated by

$$x_{i,re} = x_e + \frac{E_{i,f} - F_{i,T}}{k_e} \quad (3)$$

$$\dot{x}_{i,re} = \dot{x}_e + \frac{\dot{E}_{i,f} - \dot{F}_{i,T}}{k_e} \text{ and } \ddot{x}_{i,re} = \ddot{x}_e + \frac{\ddot{E}_{i,f} - \ddot{F}_{i,T}}{k_e} \quad (4)$$

For the simplicity of expression, let $\bar{x}_{i,0} = x_{i,0} + x_{i,off}$. Then, since $x_{i,con} = x_{i,re} - x_i = x_{i,re} - \bar{x}_{i,0} - \eta x_{i,con}$ and $\bar{x}_{i,0}$ can be assumed constant, the 1st and 2nd derivatives of $x_{i,con}$ are given by

$$\dot{x}_{i,con} = \frac{\dot{x}_{i,re}}{1+\eta} \text{ and } \ddot{x}_{i,con} = \frac{\ddot{x}_{i,re}}{1+\eta} \quad (5)$$

By combining (1), (2) and (5), the following relation is derived:

$$M_d \ddot{x}_{i,con} + B_d \dot{x}_{i,con} + k_0 x_{i,con} - k_0 \bar{x}_{i,0} = -(\eta + 1) \left\{ (1 + k_p) E_{i,f} + k_d \dot{E}_{i,f} + k_i \int_0^t E_{i,f}(\tau) d\tau \right\} \quad (6)$$

Substitution of (4) into (6) yields

$$M_d \ddot{x}_e + B_d \dot{x}_e + k_0 x_e - \frac{1}{k_e} (M_d \ddot{F}_{i,T} + B_d \dot{F}_{i,T} + k_0 F_{i,T}) = -(\eta + 1) \left\{ (1 + k_p) E_{i,f} + k_d \dot{E}_{i,f} + k_i \int_0^t E_{i,f}(\tau) d\tau \right\} - \frac{1}{k_e} (M_d \ddot{E}_{i,f} + B_d \dot{E}_{i,f} + k_0 E_{i,f}) + k_0 \bar{x}_{i,0} \quad (7)$$

Let $E(s)$, $X(s)$ and $F(s)$ denote the Laplace transforms of force tracking error $E_{i,f}$, position of glass panel x_e and desired contact force $F_{i,T}$, respectively. In the Laplace domain, (7) can be written as

$$E(s) = \frac{\Gamma(s)}{\Lambda(s)} \{F(s) - k_e X(s)\} + \frac{k_e k_0}{\Lambda(s)} \bar{x}_{i,0} \quad (8)$$

where $\Lambda(s)$ and $\Gamma(s)$ are $\Gamma(s) = M_d s^3 + B_d s^2 + k_0 s$ and $\Lambda(s) = M_d s^3 + a_0 s^2 + a_1 s + a_2$ with $\lambda = k_e(1 + \eta)$, $a_2 = k_i \lambda$, $a_1 = k_0 + \lambda(1 + k_p)$ and $a_0 = B_d + \lambda k_d$. By using the Routh stability theorem, $a_0 > 0$, $a_2 > 0$ and $a_0 a_1 - a_2 > 0$ must hold for the stability of position-based impedance control in (1) and (2). Since the positive control gains and positive scaling factor, $a_0 > 0$ and $a_2 > 0$ hold. From $B_d > 0$ and $k_0 > 0$, $a_0 a_1 - a_2 > 0$ can be expressed as

$$a_0 a_1 - a_2 = (B_d + \lambda k_d)(k_0 + \lambda(1 + k_p)) - k_i \lambda > \lambda^2 \{k_d(1 + k_p) - k_i \lambda^{-1}\} > 0 \quad (9)$$

which means that $k_d(1 + k_p) - k_i k_e^{-1}(1 + \eta)^{-1} > 0$ should hold for the stability of proposed impedance control. Since the stiffness of glass panel k_e can be assumed sufficiently large, it is easy to select the control gains and scaling factor to ensure the stability condition in (9). Also, when the desired contact force and the position of glass panel drastically change like a step, i.e., $X(s) = x_e^c/s$ and $F(s) = F_{i,T}^c/s$, the force tracking error in the steady state $E_{i,f}^{ss}$ can be proved to converge to zero by the Final value theorem under (9):

$$E_{i,f}^{ss} = \lim_{t \rightarrow \infty} E_{i,f}(t) = \lim_{s \rightarrow 0} sE(s) = \lim_{s \rightarrow 0} s \left\{ \frac{(F_{i,T}^c - x_e^c k_e)(M_d s^2 + B_d s + k_0)}{\Lambda(s)} + \frac{k_e k_0}{\Lambda(s)} \bar{x}_{i,0} \right\} = 0 \quad (10)$$

It is noteworthy that a dynamic model of manipulator is not required to ensure the force tracking ability of proposed position-based force tracking impedance control. However, a dynamic model of manipulator will play an important role in for perfect force tracking against various types of uncertainties like different shapes of glass panels and varying desired contact force, etc. In our future work, the advanced control methods will be adopted for force tracking of manipulator on the basis of its dynamic model [24]–[26].

B. OBSTACLE AVOIDANCE CONTROL

There are 15-mm raised frames between glass panels like Fig. 11(a). The cleaning device has to avoid these frames as obstacles. 2 limit switches can detect every obstacles as long as the cleaning device maintain the contact to the glass panels by the force tracking. When the cleaning device follows the cleaning trajectory (blue dotted arrows in Fig. 11(b)), the manipulator tracking the desired force for cleaning. After limit switches detect the frame like Fig. 11(c), the manipulator follows the obstacle avoiding trajectory like red dotted arrows in Fig. 11(b).

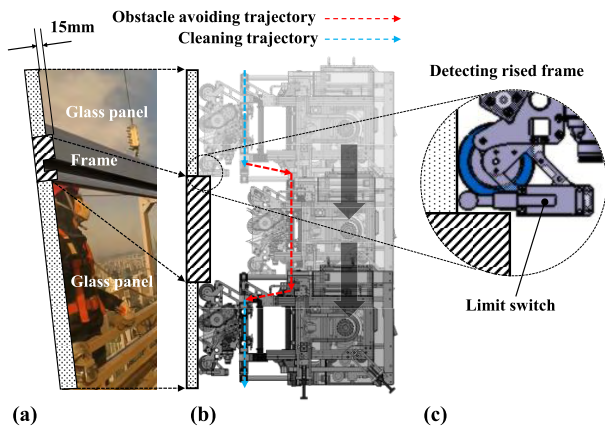


FIGURE 11. Obstacle avoidance process.

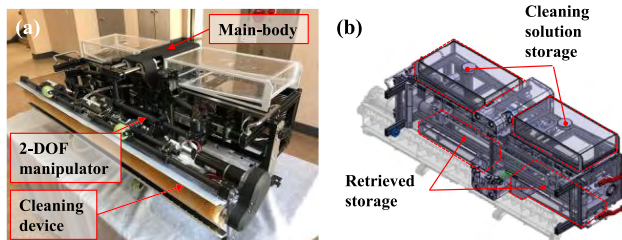


FIGURE 12. (a) Assembled prototype. (b) Cleaning solution storages of the main-body.

VI. PROTOTYPE MANUFACTURE

Fig. 12(a) shows the assembled prototype of the façade cleaning robot. The size of the prototype is 1,400 × 650 × 500 mm, and the weight is 81 kg. The weight of the separated parts of the main body and manipulator, and the cleaning device are 63 and 18 kg, respectively. For the installation, the cleaning device and manipulator can be assembled and disassembled easily by clamping devices. The cleaning solution is stored at the top of the main body, and is retrieved by vacuum suction at the bottom like Fig. 12(b). The storage space is designed to clean the vertical line of the 63-building with a single insertion (20L).

The frame structure is also developed to enable the robot to be installed on a gondola. The frame is designed to fit in a gondola, and is connected to the gondola with clamps. The robot is also connected to the frame structure using clamps. Fig. 13 shows the frame structure and the installation. It was made to fit the gondola shape of the 63-building. But every high-rise building has various shape gondola, respectively. So our frame structure can be customized to various gondola sizes and shapes. Customized frame structure also connected to the gondola using clamps.

The battery is positioned on the back-side of the frame structure. The weight of the frame structure is 40 kg without the battery (18 kg).

VII. EXPERIMENTAL ON A TEST-BENCH

Before performing a field test, we tested the performance of the cleaning robot on a test-bench. By simulating the

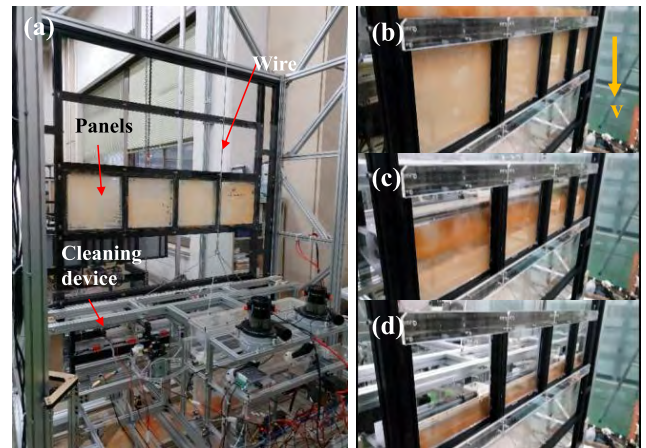


FIGURE 13. Experimental set-up used to test the cleaning device and results. (a) The experimental set-up, and (b)-(d) the process of cleaning at the start (b), mid-point (c), and finish (d).

63-building’s environment, we tested the performance of the cleaning device and manipulator independently.

First, we tested the performance of the cleaning device. Fig. 13 shows the experimental set-up used to test the performance of the cleaning device. The cleaning device is installed independently with dirty glass panels. We used four separated glass panels to investigate the data in the middle and at the edge. The cleaning device is moved by connecting it to a commercial winch with steel wire for which the speed is the same as that of the 63-building’s gondola system. As a result, the successful cleaning performance can be achieved by adjusting parameters such as the pressure of the squeegee and brushing speed, as shown in Fig. 13.

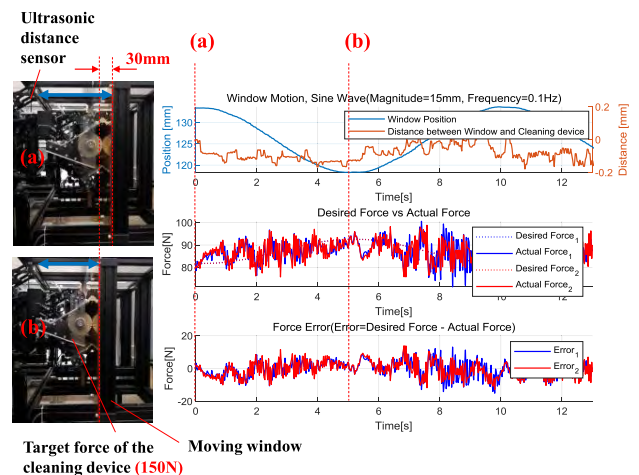


FIGURE 14. Test of the position and force control of the manipulator and the result graph when the motion of the window is sinusoidal. (a) When the window and the robot are distance, and (b) when the window and the robot are close.

Secondary, we tested the performance of the manipulator by integrating the whole system. Two performances were tested when preparing the field test. First, the position and force control performance was tested, as shown in Fig. 14.

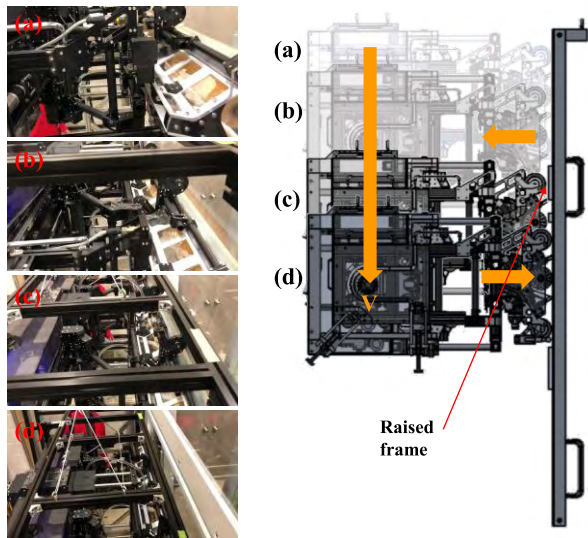


FIGURE 15. Test of the obstacle avoiding performance. (a) When the cleaning device is about to detect raised frame. (b)-(c) When the cleaning device follows obstacle avoiding trajectory. (d) When the cleaning device contacts window again.

While varying the distance, the cleaning device can be attached to the glass panel successfully with a constant contact force. The blue line on the first graph in Fig. 14 is glass panel position measured by ultrasonic sensors mounted on the main body. And the orange line is relative distance graph between glass panel and the cleaning device measured by other ultrasonic sensors mounted on the cleaning device. (see Fig. 8) Position tracking performance is confirmed because range of relative distance is much smaller than that of the moving glass panel. The desired force graph represented as dotted line on the middle graph are also sin wave because the jacobian matrix which is used for calculating desired force ($\tau_{1,d}, \tau_{2,d}$) from target force (F_{ee}, M_{ee}) is continuously varying as the manipulator configuration is varying. The force tracking performance is also confirmed in the last force error graph. RMS value of the force error are 5.10N, 5.07N respectively. Second, the obstacle avoiding performance was tested like Fig. 15. By limit switches mounted on the cleaning device, the raised frames can be detected, and the these 15-mm frames can be overcome by operating the manipulator successfully. This performance will be observed during the field test.

VIII. FIELD TEST ON 63-BUILDING

Compared with the cleaning workers, the robot is more efficient and has better cleaning performance. One person cleans one line of panel. It takes usually 30 minutes to go to the first floor. They use diatomite powder for preventing from scattering water, which is known as carcinogenic agent. They sweep their arms like wipers holding towels, so there are non-reachable spaces as shown in Fig. 19(a). But, this robot always contacts with the façade and does not need to stop,

so that the cleaning performance is much better than the workers, and this cleaning process is non-carcinogenic by using water.

We performed the field test on the 63-building. The cleaning experiments were performed on floors 2–8 of the building. After moving the cleaning robot, the frame structure, main body with manipulator, and cleaning device were installed sequentially. After that, the cleaning solution was inserted, and some pre-tests were performed on the manipulator and cleaning device. Fig. 16 shows the installed cleaning robot on the façade of the 63-building.

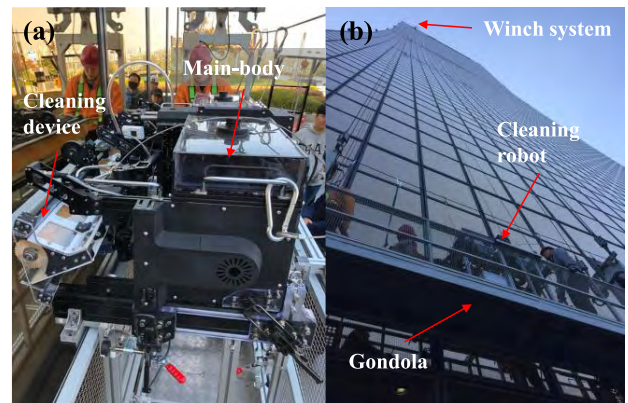


FIGURE 16. The robot attached to the gondola of the 63-building. (a) Closed view, and (b) with a gondola.

Tests were performed several times from floors 8 to 2. The vertical movement was controlled by the gondola winch (8 m/min), and the manipulator was operated to maintain the position and contact force. As a result, the cleaning performance was successfully verified, and we showed the potential for replacing the manual façade cleaning process by automated cleaning robots. Based on the sensor feedback, the 15-mm raised sections between glass panels were successfully overcome, as shown in Fig. 17.

Fig. 18 shows the measured stroke of the manipulator and the load cell data. The 15-mm raised frames between glass panels during 8 to 2 floors are overcome and the reference force of 40 N is well followed by the proposed control under various disturbances. RMS value of the force error is 6.13N during the cleaning work. The force is reduced rapidly under 0 because the robot detects and avoids the 15-mm frames, and it loses contact from the window. The negative value is because of the inertia of the end-effector. There is small overshoot but there are some rises of the force during detaching process because of unexpected hitting of the cleaning unit to the 15-mm frames.

Some problems and future research topics were realized during the field test. Some of the areas at the bottom of the glass panel cannot be cleaned because of the frames, and this is the most critical problem regarding the technical performance. Fig. 13 shows the uncleaned area of the glass panels. In the research, the cleaning performance was validated manually by cleaning experts, but it is not easy to determine

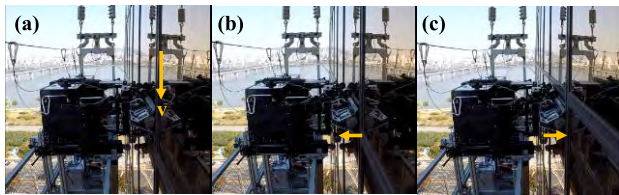


FIGURE 17. Cleaning operation and overcoming raised frames. (a) Vertical cleaning, (b) retrieval of manipulator to overcome raised frame, and (c) pushing of the manipulator to clean the next window.

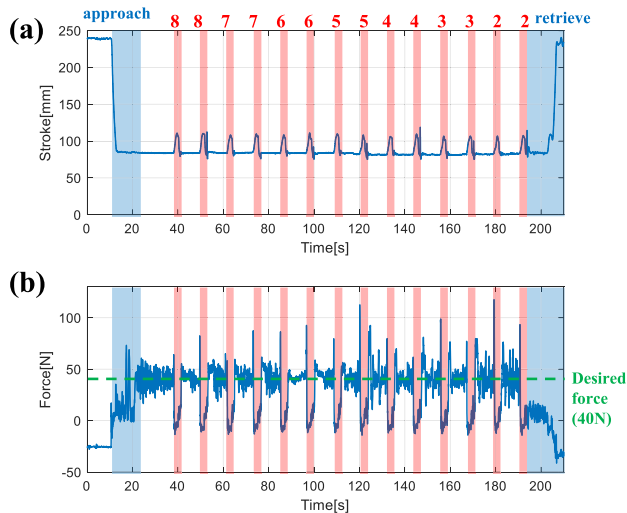


FIGURE 18. Test of the position and force control of the manipulator. (a) When the window and the robot are close, and (b) when the window and the robot are distant.

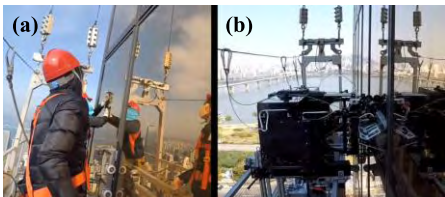


FIGURE 19. Window cleaning by (a) worker, and (b) the proposed robot.



FIGURE 20. (a) Uncleaned area of glass panel, and (b) closed view.

the cleaning performance quantitatively. There is a need for studies to standardize the façade cleaning performance based on some index using devices such as vision sensors.

IX. CONCLUSION

In this paper, we presented the results of façade cleaning experiments using a robotic solution. The experiments were performed on the 63-building in Korea. The manipulator

works to manage the position and attaching force of the cleaning device, while the cleaning device tries to clean the glass panel surface by spraying, brushing, and suctioning the cleaning solution. Based on the experimental results, we showed the potential of achieving commercial cleaning. However, some problems remain to be solved.

There is a need for future research to minimize the uncleaned area and to standardize the cleaning performance. We plan to develop an improved prototype and to perform further experiments based on the prototype. In the near future, the aim is to replace the tedious and dangerous façade cleaning work by the developed cleaning robot.

ACKNOWLEDGMENT

The authors deeply appreciate the Kumhong Company and the 63-building for their support during the field test. (*Sungkeun Yoo, Inho Joo, and Jooyoung Hong contributed equally to this work.*)

REFERENCES

- [1] SkyProCy Ltd. *SkyPro*, Cyprus. Accessed: Feb. 10, 2019. [Online]. Available: <http://www.skyprocy.com/en/company-en>
- [2] K. Seo, S. Cho, T. Kim, J. Kim, and H. S. Kim, "Design and stability analysis of a novel wall-climbing robotic platform (ROPE RIDE)," *Mechanism Mach. Theory*, vol. 70, pp. 189–208, Dec. 2013.
- [3] IPC Eagle. *HighRise Professional Window Cleaning System*. Accessed: Feb. 10, 2019. [Online]. Available: <http://www.ipceagle.com/products/highrise%E2%84%A2-professional-window-cleaning-system#.WuupHYiFOUk>
- [4] The Skyscraper Center. *The Global Tall Building Database of the CTBUH*. Accessed: Feb. 10, 2019. [Online]. Available: <http://www.skyscrapercenter.com/countries>
- [5] G. Lee, H. Kim, K. Seo, J. Kim, M. Sitti, and T. Seo, "Series of multilinked caterpillar track-type climbing robots," *J. Field Robot.*, vol. 33, pp. 737–750, Sep. 2016.
- [6] M. Eich *et al.*, "A robot application for marine vessel inspection," *J. Field Robot.*, vol. 31, no. 2, pp. 319–341, 2014.
- [7] T. Seo and M. Sitti, "Tank-like module-based climbing robot using passive compliant joints," *IEEE/ASME Trans. Mechatronics*, vol. 18, no. 1, pp. 397–408, Feb. 2013.
- [8] Y. Liu, H. Kim, and T. Seo, "AnyClimb: A new wall-climbing robotic platform for various curvatures," *IEEE/ASME Trans. Mechatronics*, vol. 21, no. 4, pp. 1812–1821, Aug. 2016.
- [9] S. M. Moon, C. Y. Shin, J. Huh, K. W. Oh, and D. Hong, "Window cleaning system with water circulation for building façade maintenance robot and its efficiency analysis," *Int. J. Precis. Eng. Manuf.-Green Technol.*, vol. 2, pp. 65–72, Jan. 2015.
- [10] T. Kim, H. S. Kim, and J. Kim, "Position-based impedance control for force tracking of a wall-cleaning unit," *Int. J. Precis. Eng. Manuf.*, vol. 17, pp. 323–329, Mar. 2016.
- [11] Kärcher, U.K. *Window Vac*. Accessed: Feb. 10, 2019. [Online]. Available: <https://www.kaercher.com/uk/home-garden/window-vac.html>
- [12] South Korea. *Windowmate*. Accessed: Feb. 10, 2019. [Online]. Available: <http://www.mywindowmate.com/>
- [13] Ecovacs Robotics, USA. *Winbot*. Accessed: Feb. 10, 2019. [Online]. Available: <https://www.ecovacs.com/us>
- [14] Taiwan. *HOBOT*. Accessed: Feb. 10, 2019. [Online]. Available: <http://www.hobot.com.tw/>
- [15] South Korea. *63-Building*. Accessed: Feb. 10, 2019. [Online]. Available: https://en.wikipedia.org/wiki/63_Building
- [16] T. Kim, Y. Jeon, S. Yoo, K. Kim, H. S. Kim, and J. Kim, "Development of a wall-climbing platform with modularized wall-cleaning units," *Autom. Construction*, vol. 83, pp. 1–18, Nov. 2017.
- [17] Japan. *BVE*. Accessed: Feb. 10, 2019. [Online]. Available: <https://www.bisoh.co.jp/product/permanent/window/>
- [18] I. Joo, J. Hong, S. Yoo, J. Kim, H. S. Kim, and T. Seo, "Parallel 2-DoF manipulator for wall-cleaning applications," *Automat. Construction*, vol. 101, pp. 209–217, 2019.

- [19] J. Hong, S. Yoo, I. Joo, J. Kim, H. S. Kim, and T. Seo, "Optimal parameter design of a cleaning device for vertical glass surfaces," *Int. J. Precis. Eng. Manuf.*, vol. 20, no. 2, pp. 233–241, 2019.
- [20] T. Kim, Y. Jeon, S. Yoo, K. Kim, H. S. Kim, and J. Kim, "Development of a wall-climbing platform with modularized wall-cleaning units," *Autom. Construction*, vol. 83, pp. 1–18, Nov. 2017.
- [21] N. Imaoka, S.-G. Roh, N. Yusuke, and S. Hirose, "SkyScraper-I: Tethered whole windows cleaning robot," in *Proc. IEEE/RSJ Int. Conf. Intell. Robots Syst. (IROS)*, Oct. 2010, pp. 5460–5465.
- [22] T. Kim, H. S. Kim, and J. Kim, "Position-based impedance control for force tracking of a wall-cleaning unit," *Int. J. Precis. Eng. Manuf.*, vol. 17, no. 3, pp. 323–329, 2016.
- [23] N. Hogan, "Impedance control: An approach to manipulation," in *Proc. IEEE Amer. Control Conf.*, Jun. 1984, pp. 304–313.
- [24] T. Kim, S. Yoo, H. S. Kim, and J. Kim, "Design and force-tracking impedance control of a 2-DOF wall-cleaning manipulator using disturbance observer and sliding mode control," in *Proc. IEEE Int. Conf. Robot. Autom. (ICRA)*, Brisbane, QLD, Australia, May 2018, pp. 1–9.
- [25] S. Zhang, Y. Dong, Y. Ouyang, Z. Yin, and K. Peng, "Adaptive neural control for robotic manipulators with output constraints and uncertainties," *IEEE Trans. Neural Netw. Learn. Syst.*, vol. 29, no. 11, pp. 5554–5564, Nov. 2018.
- [26] W. He, Y. Ouyang, and J. Hong, "Vibration control of a flexible robotic manipulator in the presence of input deadzone," *IEEE Trans. Ind. Informat.*, vol. 13, no. 1, pp. 48–59, Feb. 2017.
- [27] H. Gao, W. He, C. Zhou, and C. Sun, "Neural network control of a two-link flexible robotic manipulator using assumed mode method," *IEEE Trans. Ind. Informat.*, vol. 15, no. 2, pp. 755–765, Feb. 2018.



SUNGKEUN YOO received the B.S. degree in mechanical and aerospace engineering from Seoul National University, in 2014, where he is currently pursuing the Ph.D. degree in mechanical engineering. His research interest includes robot mechanism design.



INHO JOO received the B.S. degree in robotics from Kwangwoon University, in 2017. He is currently pursuing the M.S. degree in mechanical engineering with Seoul National University. His research interest includes robot mechanism design.



JOOYOUNG HONG received the B.S. degree in mechanical engineering from Yonsei University, in 2018. He is currently pursuing the M.S. degree in mechanical engineering with Seoul National University. His research interest includes robot mechanism design.



CHANGMIN PARK received the B.S. degree in mechanical engineering from Youngnam University, in 2017. He is currently pursuing the M.S. degree in mechanical engineering with Hanyang University. His research interest includes robot mechanism design.



JONGWON KIM received the B.S. degree in mechanical engineering from Seoul National University, South Korea, in 1978, the M.S. degree in mechanical and aerospace engineering from the Korea Advanced Institute of Science and Technology, South Korea, in 1980, and the Ph.D. degree in mechanical engineering from the University of Wisconsin–Madison, USA, in 1987. He is currently a Professor with the School of Mechanical and Aerospace Engineering, Seoul National University. His current research interests include parallel mechanisms, Taguchi methodology, and field robots.



HWA SOO KIM (M'15) received the B.S. and Ph.D. degrees in mechanical engineering from Seoul National University, South Korea, in 2000 and 2006, respectively. From 2007 to 2008, he was a Postdoctoral Researcher with the Laboratory for Innovations in Sensing, Estimation and Control, University of Minnesota, MN, USA. He is currently an Associate Professor with the Department of Mechanical System Engineering, Kyonggi University. His current research interests include design, modeling, and control of various mobile platforms.



TAEWON SEO (M'10) received the B.S. and Ph.D. degrees from the School of Mechanical and Aerospace Engineering, Seoul National University, South Korea. He was a Postdoctoral Researcher with the Nanorobotics Lab, Carnegie Mellon University, a Visiting Professor with the Biomimetic Millisystems Lab, University of California at Berkeley, and an Assistant Professor with the School of Mechanical Engineering, Yeungnam University, South Korea. He is currently an Associate Professor with the School of Mechanical Engineering, Hanyang University, South Korea. His research interests include robot design, analysis, control, optimization, and planning. He received the Best Paper Award of the IEEE/ASME TRANSACTION ON MECHATRONICS, in 2014. He is a Technical Editor of the IEEE/ASME TRANSACTION ON MECHATRONICS and an Associate Editor of the IEEE ROBOTICS AND AUTOMATION LETTERS and *Intelligent Service Robotics*.

...